Neutrinos from failed supernovae at future water and liquid argon detectors

James G. Keehn and Cecilia Lunardini

Phys. Rev. D **85**, 043011 — Published 14 February 2012

DOI: 10.1103/PhysRevD.85.043011

Neutrinos from failed supernovae at future water and liquid argon detectors

James G. Keehn[1,2] and Cecilia Lunardini[1,3]

[1]*Arizona State University, Tempe, AZ 85287-1504, USA*

[2]*Missouri University of Science and Technology, Rolla, MO 65409, USA*

[3]*RIKEN BNL Research Center, Brookhaven National Laboratory, Upton, NY 11973, USA*

Abstract

We discuss the diffuse flux of electron neutrinos and antineutrinos from cosmological *failed supernovae*, stars that collapse directly into a black hole with no explosion. This flux has a hotter energy spectrum compared to the flux from regular, neutron-star forming collapses and therefore it dominates the total diffuse flux from core collapses above 20-45 MeV of neutrino energy. Reflecting the features of the originally emitted neutrinos, the flux of ν_e and $\bar{\nu}_e$ at Earth is larger when the survival probability of these species is larger, and also when the equations of state of nuclear matter are stiffer. In the 19-29 MeV energy window, the flux from failed supernovae is susbtantial, ranging from $\sim$7% to a dominant fraction of the total flux from all core collapses. It can be as large as $\phi_{\bar{e}}^{BH} = 0.38$ s^{-1}cm^{-2} for $\bar{\nu}_e$ and as large as $\phi_e^{BH} = 0.28$ s^{-1}cm^{-2} for ν_e, normalized to a local rate of core collapses of $R_{cc}(0) = 10^{-4}$ yr^{-1}Mpc^{-3}. In 5 years, a 0.45 Mt water Cherenkov detector should see $\sim 5 - 65$ events from failed supernovae, while up to ~ 160 events are expected for the same mass with Gadolinium added. A 0.1 Mt liquid argon experiment should record $\sim 1 - 11$ events. Signatures of neutrinos from failed supernovae are the enhancement of the total rates of events from core collapses (up to a factor of ~ 2) and the appearance of high energy tails in the event spectra.

PACS numbers: 97.60.Bw,14.60.Pq

I. INTRODUCTION

Neutrinos are unique probes of the physics of collapsing stars (supernovae). Diffusing from the dense region surrounding the collapsed stellar core, they can deliver first hand information on the collapse of their stars, on the physics of matter near nuclear density and on the propagation of neutrinos from such high densities to the interstellar space and to detectors on Earth.

The physics potential of neutrinos from supernovae has been studied only minimally due to the scarcity of data. These are limited to handful of events from SN1987A [1, 2], which was the only recent supernova close enough for its neutrino flux to be detectable. While the rarity of nearby supernovae seems an insurmountable problem, a new phase of data taking is expected to begin with the detection of the *diffuse supernova neutrino flux* (or background, DSNB), on which only upper limits exist [3–6]. Tiny but continuous in time, the diffuse flux will give tens to hundreds of events in a few years at future Mt scale detectors, ensuring constant progress for decades.

Besides the practical advantages, the diffuse flux has a theoretical value of its own: indeed, it has the unique potential to probe the entire supernova population of the universe in its diversity. An important advancement in this direction is the study of the neutrino flux from *failed supernovae*, stars that collapse directly into a black hole with no explosion and no significant emissions other than neutrinos and gravitational waves. These direct black hole-forming collapses are rare; they are estimated to account for less than $\sim 22\%$ of all collapses [7, 8]. The physics of failed supernovae were modeled numerically in a number of works, including [7, 9–14], which predicted the emission of a neutrino flux with a higher luminosity and average energy compared to the flux from regular, neutron star-forming collapses.

In [8] this result was used to make the first calculation of the diffuse neutrino flux from failed supernovae. The main result was the possibility that, due to their higher energetics, failed supernovae might contribute substantially to the DSNB, with an enhancement of the total flux and event rate in water detectors of up to $\sim 100\%$.

The possibility to detect neutrinos from failed supernovae in the form of a diffuse flux has several interesting implications. Experimentally, the enhancement of the total flux is attractive because it means that a detection might be closer in time and within the reach of the next phase of SuperKamiokande, especially in the configuration with Gadolinium

[15]. Theoretically, detecting the diffuse flux would make it possible to learn about direct black hole-forming collapses, specifically by constraining their energetics and cosmological rate. This opportunity is especially precious, considering that failed supernovae are virtually invisible to telescopes [71]. The published SuperKamiokande neutrino data already constrain the rate of failed supernovae [16]. A new, preliminary, analysis from the SuperKamiokande collaboration [17, 18] considers the neutrino flux from failed supernovae, and limits it to about a factor of two from the most optimistic predictions. Neutrinos from failed supernovae can also increase the amount of Technetium 97 (^{97}Tc) that accumulates in Molybdenum ores over millions of years due to solar and galactic supernova neutrino irradiation [19]. It was observed that they also enhance the proposed neutrino-based mechanisms to create amino acid enantiomerism [20].

In this paper we elaborate further on the theme of the diffuse neutrino flux from failed supernovae, with a focus on its dependence on the relevant parameters and on its signatures at the next generation of neutrino detectors with 0.1 - 1 Mt masses. Specifically, we consider a Mt water Cherenkov detector and a 0.1 Mt liquid argon (LAr) experiment. Our results for water Cherenkov detectors elaborate on those of ref. [8], while the discussion of the potential of liquid argon detectors is presented here for the first time. The advent of liquid argon technology will be a revolution for the study of supernova neutrinosdue to its strong sensitivity to electron neutrinos, which complements the sensitivity of water detectors to antineutrinos. A mass of 0.1 Mt is considered to be the minimum mass required to have any sensitivity to diffuse supernova neutrinos. We will show that this configuration might be particularly suited for neutrinos from failed supernovae: their higher energies imply a larger detection cross section compared to neutrinos from neutron-star forming collapses, and their event energy spectrum might peak above the background of solar neutrinos. The enhancement of the event rate due to failed supernovae increases the potential of discovery of the DSNB during the earliest phase of the liquid argon technology development.

The paper opens with generalities on neutrinos from failed supernovae, their expected flux at Earth and basics of their detection and relevant backgrounds (sec. II). We then give results for fluxes and event rates in the antineutrino channel (sec. III) and the neutrino channel (sec. IV). In sec. VI the results are discussed and summarized.

II. GENERALITIES

A. Failed supernovae and their neutrinos

Core collapse occurs for stars with mass $M \gtrsim 8M_\odot$ (with $M_\odot = 1.99 \cdot 10^{30}$ Kg, the mass of the Sun) at an average rate of $R_{cc}(0) \sim 10^{-4}$ Mpc^{-3}yr^{-1} today [21] and of

$$R_{cc}(z) \propto \begin{cases} (1+z)^\beta & z < 1 \\ (1+z)^\alpha & 1 < z < 4.5 \\ (1+z)^\gamma & 4.5 < z \end{cases} \quad (1)$$

at redshift z, with $\beta \simeq 3$, $\alpha \simeq 0$ and $\gamma \simeq -8$ [21]).

For $M = 8 - 25M_\odot$ the collapse leads to an explosion, followed by the formation of a neutron star [22]. Considering that stars are distributed in mass as $\phi(M) \propto M^{-2.35}$ [23], one gets that these Neutron Star Forming Collapses (NSFCs) are a fraction $f_{NS} \simeq 0.78$ of the total. They emit neutrinos in comparable amounts in the six species: $\nu_e, \bar{\nu}_e, \nu_\mu, \bar{\nu}_\mu, \nu_\tau, \bar{\nu}_\tau$ ($\nu_\mu, \bar{\nu}_\mu, \nu_\tau, \bar{\nu}_\tau$=$\nu_x$ from here on). At the production site, the flux in each species w, differential in energy, can be described as [24]:

$$F_w^0 \simeq \frac{(1+\alpha_w)^{1+\alpha_w} L_w}{\Gamma(1+\alpha_w) {E_{0w}}^2} \left(\frac{E}{E_{0w}}\right)^{\alpha_w} e^{-(1+\alpha_w)E/E_{0w}}, \quad (2)$$

where $\Gamma(x)$ stands for the Gamma function. Here α_w controls the spectral shape, L_w is the time integrated luminosity and E_{0w} is the average energy. Here we will use typical values [24]: $E_{0e} = 9$ MeV, $E_{0\bar{e}} = 15$ MeV, $E_{0x} = 18$ MeV, $L_e = L_{\bar{e}} = L_x = 5 \cdot 10^{52}$ ergs, $\alpha_e = \alpha_{\bar{e}} = 3.5$ and $\alpha_x = 2.5$. For these, the fluxes $F_e^0, F_{\bar{e}}^0, F_x^0$ are illustrated in fig. 1 (dashed lines).

While neutron star-forming collapses have been studied in detail, the evolution of higher mass stars is more uncertain. For $M \sim 25 - 40\ M_\odot$ (13% of the total) a weaker explosion should occur, with a black hole formed by fallback [22, 25]. Stars with $M \gtrsim 40\ M_\odot$ (a 9% fraction), would instead collapse into a black hole directly. Simulations of such Direct Black Hole Forming Collapses (DBHFCs) [7, 9–12] show an emitted neutrino flux that is more energetic and more luminous than the NSFC case as a result of the rapid contraction of the protoneutron star (see e.g., [7]). Furthermore, the ν_e and $\bar{\nu}_e$ fluxes are especially luminous due to the capture of electrons and positrons on nucleons.

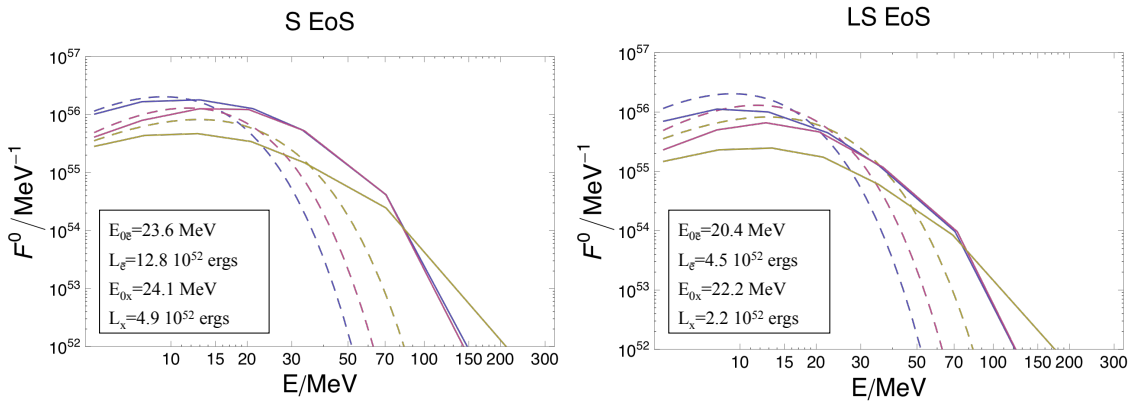

FIG. 1: Neutrino fluxes at production inside the star for direct black hole-forming collapses (solid, from [13]) , and neutron star-forming collapses (dashed, Eq. (2)). In both cases, the curves from upper to lower at 10 MeV correspond to ν_e, $\bar{\nu}_e$, ν_x. For direct black hole-forming collapses the neutrino spectra are shown for the Shen et al. (left panel) and Lattimer-Swesty (right) equations of state. For each, the neutrino luminosities and average energies are given (insets). See text for details.

A "stiffer" equation of state (EoS) of nuclear matter [7] and/or a smaller accretion rate of matter on the protoneutron star [11] correspond to more luminous and hotter neutrino fluxes. Here we take the fluxes from DBHFCs from fig. 5 of Nakazato et al. [13], using the same linear interpolation of numerically calculated points (which underestimates the DSNB in the SuperKamiokande energy window by about 10-20% [8]). They are are shown in fig. 1. These fluxes were obtained for the $40M_\odot$ progenitor in [26] with the stiffer Shen et al. (S) EoS [27] (incompressibility $K = 281$ MeV) and the softer Lattimer-Swesty (LS) EoS [28] (with $K = 180$ MeV [13]). For the different progenitors considered in [13] results appear unchanged for the S EoS, while for the LS one the luminosity and average energy may be lower by a factor of two and by 10-20% respectively.

Flavor oscillations modify the flavor composition of the neutrino flux in a way that is similar, in its generalities, for NSFCs and DBHFCs, as was shown in an initial study [13]. After oscillations the fluxes of the ν_e and $\bar{\nu}_e$ species are admixtures of the original fluxes of the different flavors:

$$F_e = pF_e^0 + (1-p)F_x^0 \quad , \tag{3}$$

$$F_{\bar{e}} = \bar{p}F_{\bar{e}}^0 + (1-\bar{p})F_x^0 \ , \tag{4}$$

where the probabilities p and $\bar{p}$ depend on the structure of the neutrino mass spectrum and mixing, and on refraction effects due to neutrino-neutrino and to neutrino-electron interaction, with the latter producing two MSW resonances inside the star [29]. A very general result – valid if turbulence effects are negligible – is that p and $\bar{p}$ vary in the intervals [30]:

$$\begin{aligned} p &= 0 - \sin^2\theta_{12} \simeq 0 - 0.32 \ , \\ \bar{p} &= 0 - \cos^2\theta_{12} \simeq 0 - 0.68 \ . \end{aligned} \tag{5}$$

Their energy dependence is generally smooth due to the energy dependence of the transition probability in the highest density MSW resonance (see e.g., [31]). An exception is the recently studied "spectral swap", a step-like structure in the probabilities as functions of energy caused by neutrino-neutrino interaction (see e.g., [32–36] and the review [37] and references therein). For the inverted mass hierarchy a sharp, single swap should appear in the ν_e spectrum at the critical energy E_c defined as [34]:

$$\int_{E_c}^{\infty} (F_e^0 - F_x^0) = \int_0^{\infty} (F_{\bar{e}}^0 - F_x^0) \ , \tag{6}$$

and the probability p is then given by:

$$p \simeq \begin{cases} \sin^2\theta_{12} \simeq 0.32 & (E < E_c) \\ 0 & (E > E_c) \end{cases} \tag{7}$$

Typical values of E_c are $E_c \simeq 3-10$ MeV [38]; for our set of parameters we find $E_c \simeq 8$ MeV for NSFCs and $E_c \simeq 12$ MeV for DBHFCs using both equations of state. Multiple other swaps could also appear in both the ν_e and $\bar{\nu}_e$ channels in a way that is highly dependent on the original neutrino fluxes and on the mass hierarchy [39–41].

A study of the MSW resonances only (no neutrino-neutrino effects) for DBHFCs [13] (see also [42]) indicates that the oscillation pattern is the same for both collapse types in the intervals $\sin^2\theta_{13} \gtrsim 3\cdot 10^{-4}$ or $\sin^2\theta_{13} \lesssim 3\cdot 10^{-6}$, where the higher density MSW resonance is completely adiabatic or completely non-adiabatic. In this case the probabilities are energy-independent and take their extreme values in eq. (5). While swap effects have not been studied for DBHFCs, we expect that the picture with a single swap, eq. (7), should be valid since it is a typical occurence when $F_x^0 \lesssim F_e^0, F_{\bar{e}}^0$ [40].

For generality, here we follow ref. [8] and limit our discussion to energy-independent permutation parameters that are equal for both collapse types. We give results only for

the extremes of the intervals of the permutation parameters, Eq. (5): from these one can easily derive fluxes and event rates for intermediate values. The approximation of energy-independent permutation should be adequate in the energy windows relevant for the DSNB detection ($E \gtrsim 11 - 20$ MeV, see sec. II B): indeed, we have checked that the largest energy modulations due to the MSW resonance cause an effect at the level of 20% or less on the DSNB spectrum, which is negligible compared to other uncertainties in the problem. Moreover, our calculated values of E_c produce effects on the DSNB that fall below typical windows of detection. Still, in sec. II B we briefly discuss the effect of spectral swaps.

B. Fluxes at Earth: signal and backgrounds

Following ref. [8], we model the neutrino fluxes from NSFCs and DBHFCs, and the total diffuse flux for a schematic two-population scenario, with a fraction f_{NS} ($f_{BH} = 1 - f_{NS}$) of identical neutrino emitters of the NSFC (DBHFC) type. The total diffuse $\bar{\nu}_e$ flux at Earth, differential in energy and area, is:

$$\begin{aligned}
&\Phi_{\bar{e}}(E) = \Phi_{\bar{e}}^{BH} + \Phi_{\bar{e}}^{NS} \ , \\
&\Phi_{\bar{e}}^{BH} = \frac{c}{H_0}(1 - f_{NS}) \int_0^{z_{max}} R_{cc}(z) F_{\bar{e}}^{BH}(E(1+z)) \frac{dz}{\sqrt{\Omega_m (1+z)^3 + \Omega_\Lambda}} \ , \\
&\Phi_{\bar{e}}^{NS} = \frac{c}{H_0} f_{NS} \int_0^{z_{max}} R_{cc}(z) F_{\bar{e}}^{NS}(E(1+z)) \frac{dz}{\sqrt{\Omega_m (1+z)^3 + \Omega_\Lambda}} \ ,
\end{aligned} \tag{8}$$

where $\Omega_m = 0.3$ and $\Omega_\Lambda = 0.7$ are the fractions of the cosmic energy density in matter and dark energy, c is the speed of light and H_0 is the Hubble constant. An analogous expression holds for the ν_e diffuse flux Φ_e. In what follows the values $R_{cc}(0) = 10^{-4}$ Mpc^{-3}yr^{-1}, $\beta = 3.28$, $\alpha = 0$ and $z_{max} = 4.5$ [21] will be used (results depend weakly on z_{max}, at the level of $\sim 7\%$ or less for $z_{max} \gtrsim 3$ [43]). We take the interval $f_{NS} = 0.78 - 0.91$, corresponding to a mass of $25 - 40\ M_\odot$ as the upper limit for neutron star-forming collapses, as a way to parametrize the uncertainty in the neutrino fluxes in the region of transition between robust, neutron-star forming explosions and direct black hole formation. Most of this uncertainty is due to the poorly studied neutrino emission for black hole formation by fallback (see sec. V). There are also uncertainties in the minimum mass required for direct black hole formation: a value as low as $\sim 17 - 20 M_\odot$ is compatible with observations of progenitors

of type IIP supernovae [44], while numerical studies indicate larger minimum masses, with wide variations associated with the star's metallicity and rotation (see e.g., [45]).

An example of the resulting diffuse neutrino fluxes is given in fig. 2, which shows $\Phi_{\bar{e}}^{BH}$ and $\Phi_{\bar{e}}^{NS}$ as well as the contributions to each from different redshift bins [72]. The parameters that maximize $\Phi_{\bar{e}}^{BH}$ above 20 MeV have been chosen (see caption). While a detailed discussion is deferred to secs. III and IV, here we observe the main differences between the two fluxes: reflecting the features of the original spectra at production, $\Phi_{\bar{e}}^{BH}$ has a more energetic spectrum so that, in spite of the rarity of failed supernovae, it dominates above 20 MeV or so.

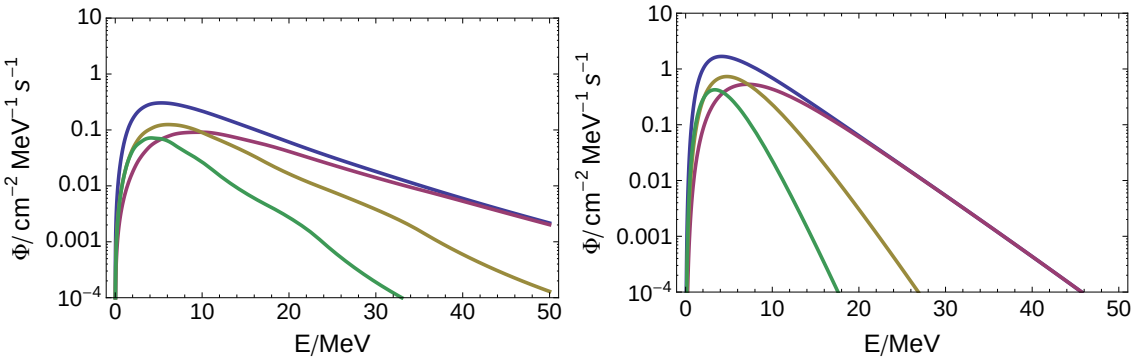

FIG. 2: The diffuse flux of $\bar{\nu}_e$ from black hole-forming collapses (left panel) and from neutron star-forming collapses (right panel) from different bins of redshift, z. From lower to upper curves at 20 MeV: $2 \leq z < 3$, $1 \leq z < 2$, $0 \leq z < 1$, and the total from all redshifts. We used the S EoS, $\bar{p} = 0.68$ and $f_{NS} = 0.78$.

From the contributions of each redshift bin we see that, as expected, the flux from more distant collapses accumulates at lower energies due to the redshift of energy, and so generally at energies relevant for detection ($E \gtrsim 10 - 20$ MeV) the flux from sources with $z < 1$ dominates. Still, for DBHFCs the flux from higher redshifts ($z \gtrsim 1$) is substantial: at 10 MeV (20 MeV) it is about 58% (32%) of the total from failed supernovae. For other combinations of parameters the fraction varies in the interval 52-58% (30-40%).

In contrast, the analogous calculation for neutron star-forming collapses gives 40% (9%) (of the total from neutron star-forming collapses) at 10 MeV (20 MeV).

The larger cosmological component of the failed supernova flux is explained by the more energetic original neutrino spectra. In principle, its implications are profound: if seen, this flux can probe the rate of failed supernovae beyond $z \simeq 1$. This is the limit of current

supernova surveys, which are not sensitive to direct black hole-forming collapses in any case.

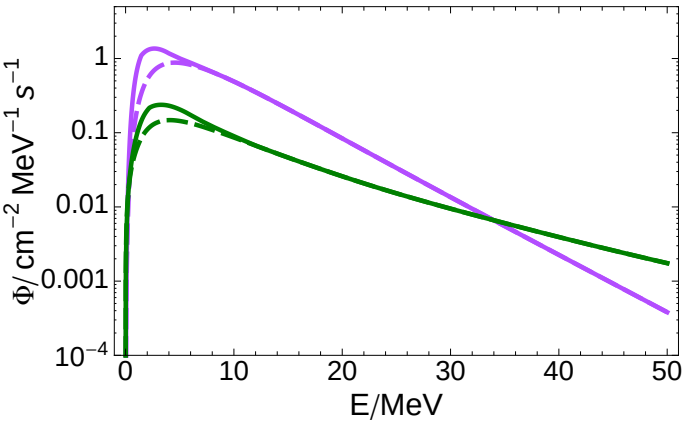

FIG. 3: ν_e fluxes from direct black hole-forming collapses (lower curves at 10 MeV) and from neutron star-forming collapses (upper curves) for $p = 0$ (dashed lines) and for the step-like probability in eq. (7) (solid). The swap energies are $E_c = 12.1, 8.0$ MeV for the the two fluxes respectively. We used the S EoS and $f_{NS} = 0.78$.

Summing over many sources at different redshifts smears out potentially interesting oscillation effects, so that only dramatic features affecting the original fluxes might appear in the DSNB. In fig. 3 we give an example of how Φ_e^{BH} and Φ_e^{NS} are modified by the spectral swap, eq. (7), assuming that a single swap is realized according to eq. (6). Due to the smearing, the effect of the swap is a smooth spectral distortion at $E < E_c$. In this interval the flux is larger compared to the case of constant $p = 0$. This is due to the larger survival of the original ν_e flux, which is the dominant component at these energies. When compared with the case where $p = 0.32$, instead, the step causes a suppression of the flux in the same interval. We do not discuss the swap effects in detail because the spectral distortion falls below detectable energies. The question should be reexamined, however, when a detailed picture of neutrino-neutrino refraction in failed supernovae becomes available.

The potential to detect diffuse neutrinos from core collapses is strongly influenced by backgrounds, which determine the *energy window* of sensitivity (defined as the interval where the DSNB exceeds other neutrino fluxes) and the statistical significance of a signal. Several neutrino fluxes of other origin constitute ineliminable backgrounds for water and LAr experiments; they are shown in fig. 4. Since water detectors are mostly sensitive to $\bar{\nu}_e$s,

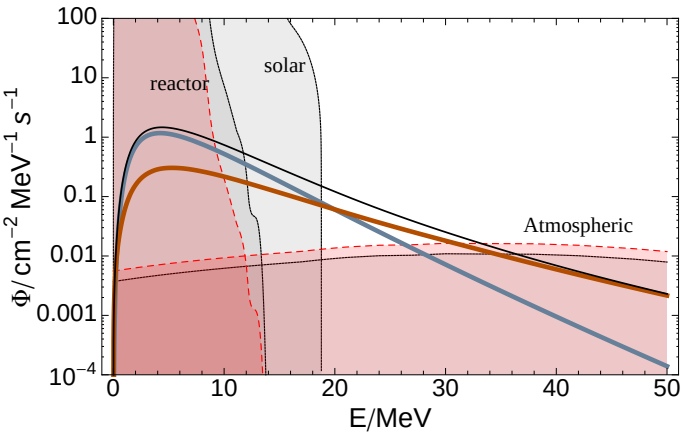

FIG. 4: Signal and background fluxes. The atmospheric and reactor fluxes are shown for the Kamioka (solid, gray) and Homestake (dashed, red) sites. The atmospheric fluxes of ν_e and $\bar{\nu}_e$ (from [46]) are very similar, so only one of them is plotted. The calculations of the background fluxes include oscillation effects, which are responsible for the visible modulation of the reactor spectrum. The signal flux plotted refers to the $\bar{\nu}_e$ channel, with the S EoS, $p = 0.68$ and $f_{NS} = 0.78$. From the lower to upper curves at 40 MeV: the flux from neutron star-forming collapses, the flux from direct black hole-forming collapses and the total flux.

their backgrounds are $\bar{\nu}_e$ fluxes from the atmosphere and from reactors. The atmospheric $\bar{\nu}_e$s are truly indistinguishable from diffuse supernova neutrinos because they have the same energy range and the same isotropic distribution in space. Their flux exceeds the DSNB typically above 30-40 MeV, thus restricting the experimental sensitivity to this range. The restriction is stronger for detectors closer to the Earth's poles, where the atmospheric flux is larger. Fig. 4 illustrates this, showing the atmospheric $\bar{\nu}_e$ flux, taken from the FLUKA group [46], at Kamioka and Homestake; the second location has a higher flux by a factor ~ 1.5, which results in a restriction of the energy window by 2-4 MeV.

For the same two locations the reactor flux is shown in fig. 4 (from [47]). It is stronger at Kamioka, reflecting the high concentration of nuclear reactors in Japan, and weaker by a factor ~ 24 at Homestake [48, 49]. It restricts the experimental sensitivity to the DSNB to neutrino energies higher than ~ 10 MeV (~ 12 MeV) at Homestake (Kamioka). Reactor neutrino events could be distinguished in principle from their direction; conceptual studies exist on this in the context of geoneutrino detection [50, 51], but their effectiveness for the DSNB is unclear at this time.

LAr detectors are mostly sensitive to electron neutrinos, and therefore solar and atmospheric ν_e fluxes are the main backgrounds for them. The atmospheric ν_e flux is very similar to the $\bar{\nu}_e$ one at these energies, so the considerations above apply. The flux from the *hep* process in the Sun prevents studying the DSNB below ~ 18 MeV, unless a method is devised to distinguish it using directional information [73]. The solar neutrino flux is plotted in fig. 4; it is from the BPS05 model [52] with the inclusion of oscillation effects as in [19].

Clearly, the energy window widens for a larger DSNB, and therefore a strong flux from failed supernovae is advantageous for signal to background discrimination. For our parameters of choice and the largest DBHFCs flux, we find that the window is $\sim 12 - 36$ MeV for a water detector at Kamioka and $\sim 9 - 32$ MeV for one at Homestake. Instead, if the flux from DBHFCs is negligible, the window is $\sim 12 - 29$ MeV and $\sim 9 - 27$ MeV in the two cases respectively. These windows refer to the ideal case in which other, non-neutrino, backgrounds can be neglected. In practice, however, water detectors are limited by other backgrounds that will be summarized next.

C. Neutrino detection

We consider a representative scenario with a water Cherenkov detector and a LAr detector of 0.45 Mt and 0.1 Mt fiducial masses respectively, as envisioned for the next generation of underground laboratories. We discuss each briefly and refer to recent reviews [53] for more details.

For a water Cherenkov detector the main detection channel is inverse beta decay:

$$\bar{\nu}_e + p \to n + e^+ \ , \tag{9}$$

which dominates the event rate due to to the larger cross section compared to other relevant processes. Here we consider only inverse beta decay, with the cross section from [54], and present results in terms of the positron energy $E_e \simeq E - 1.3$ MeV. We consider a representative detection efficiency of 90%. Besides atmospheric and reactor neutrinos, a water detector suffers large backgrounds from spallation and invisible muons, which we model following Fogli et al. [55]. Spallation products motivate limiting the search to the window $E_e \geq 18$ MeV ($E \geq 19.3$ MeV) at SuperKamiokande, while invisible muon events are included in the analysis and exceed the signal [3]. Current SuperKamiokande data give a

stringent upper limit on the $\bar{\nu}_e$ component of the DSNB [3, 6] [74] :

$$\phi_{\bar{e}}(E)(E > 19.3 \text{ MeV}) < 1.4 - 1.9 \text{ cm}^{-2}\text{s}^{-1} \quad \text{at } 90\%\text{C.L.} , \tag{10}$$

where the interval of values accounts for varying neutrino spectra. Although our main focus is on Mt class detectors, we will discuss how this limit constrains the flux of neutrinos from failed supernovae (sec. III).

If Gadolinium is dissolved in the water, as in the proposed GADZOOKS design [15], neutron tagging becomes possible, so that spallation can be almost completely subtracted and the invisible muon background effectively reduces by a factor of ~ 5 [15]. This allows to search for the DSNB in the whole energy window determined by reactor and atmospheric neutrinos. In sec. III we will give results for this larger window, as well as for the one relevant to pure water.

In LAr the largely dominant detection channel is charged current ν_e scattering:

$$\nu_e + {}^{40}Ar \rightarrow X + e^- , \tag{11}$$

where X stands for any of the possible products. The emitted electron is detected by the ionization track it produces in the liquid Argon. We model the process (11) following ref. [56] and use ref. [57] for the cross section. The energy of the emitted electron differs from that of the incoming neutrino by $\sim$ 3-4 MeV depending on the nuclear transition taking place [56]. Since detailed information on the spectrum of these transitions is not available, however, here event rates will be discussed in terms of neutrino energy. For generality, we use a 100% detection efficiency. We consider only the solar and atmospheric backgrounds, under the assumption that events of other nature can be effectively identified and subtracted; this is being investigated in the intense R&D work that is ongoing at this time.

In the reminder of the paper we consider all backgrounds for the Kamioka site; results for the Homestake location can be inferred using the rescaling factors in sec. II B as well as fig. 4 for estimating the energy window.

III. ANTINEUTRINOS: FLUX AND EVENT RATES IN WATER

A. $\bar{\nu}_e$ flux

Fig. 5 shows the $\bar{\nu}_e$ fluxes from NSFCs and DBHFCs, as well as the corresponding integrated fluxes in the energy windows relevant to pure water and water with Gadolinium.

As expected, the diffuse fluxes reflect the features of the originally produced fluxes of each supernova type. The diffuse flux from failed supernovae has a harder spectrum compared to the flux from neutron star-forming collapses, and is larger for the S EoS. Above 20 MeV, $\Phi_{\bar{e}}^{BH}$ is highest for the S EoS, $f_{NS} = 0.78$ and $\bar{p} = 0.68$. For this "best case scenario", the contribution from failed supernovae is dominant in the interval of sensitivity of pure water, reaching ~ 0.07 cm^{-2}s^{-1}MeV^{-1} at 20 MeV and falling almost exponentially at higher energy. This is the result already highlighted in [8]: the diffuse flux from failed supernovae could be large and therefore detectable, with interesting implications for the study of direct black hole formation.

Results vary substantially with the parameters, however. An uncertainty of a factor of ~ 2 is associated with the fraction of black hole-forming collapses, $1 - f_{NS} = 0.09 - 0.22$, and a lower $\Phi_{\bar{e}}^{BH}$ is expected for the LS EoS and for the total flavor permutation $\bar{p} = 0$. This latter feature is peculiar of failed supernovae (the opposite is realized for neutron star-forming collapses), and is due to the especially luminous and energetic original $\bar{\nu}_e$ flux. When all parameters conspire to suppress it, $\Phi_{\bar{e}}^{BH}$ is small, exceeding the flux from NSFCs only above $\sim$45 MeV where the atmospheric background dominates by one order of magnitude.

Let us now discuss the fluxes integrated over the water detector energy window, $E \sim 19.3 - 29.3$ MeV. In this interval the failed supernova flux varies by about one order of magnitude, from 0.03 cm^{-2}s^{-1} to 0.38 cm^{-2}s^{-1}, corresponding to $\sim 6-57\%$ of the total flux. The latter is enhanced by up to a factor ~ 2.3 compared to neutron star-forming collapses only, and can be as high as 0.67 cm^{-2}s^{-1}. The flux in the open interval $E \geq 19.3$ MeV can reach 0.89 cm^{-2}s^{-1}, about a factor of two away from the most conservative SuperKamiokande limit, eq. (10). This indicates the exciting possibility of detection in the near future at SuperKamiokande or GADZOOKS, before the advent of more massive detectors.

The SuperKamiokande limit can be used to constrain the space of parameters [16]. For example, if we compare this limit to the total predicted flux, $\Phi_{\bar{e}}^{BH} + \Phi_{\bar{e}}^{NS}$, we get a constraint

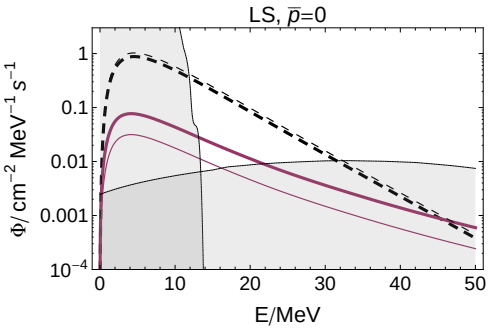

SuperK : 19.3 – 29.3 MeV

fNS	flux NS	flux BH	flux total
0.78	0.44	0.07	0.51
0.91	0.51	0.03	0.54

GADZOOKS: 11.3 – 29.3 MeV

fNS	flux NS	flux BH	flux total
0.78	2.15	0.25	2.39
0.91	2.5	0.1	2.6

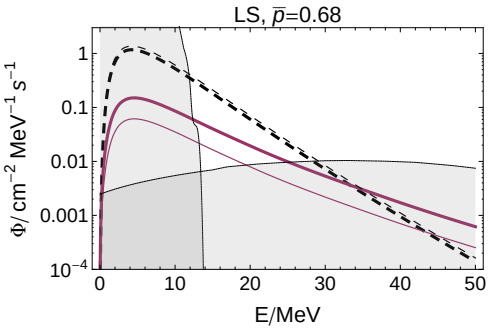

SuperK : 19.3 – 29.3 MeV

fNS	flux NS	flux BH	flux total
0.78	0.29	0.12	0.41
0.91	0.34	0.05	0.38

GADZOOKS: 11.3 – 29.3 MeV

fNS	flux NS	flux BH	flux total
0.78	1.82	0.44	2.26
0.91	2.12	0.18	2.3

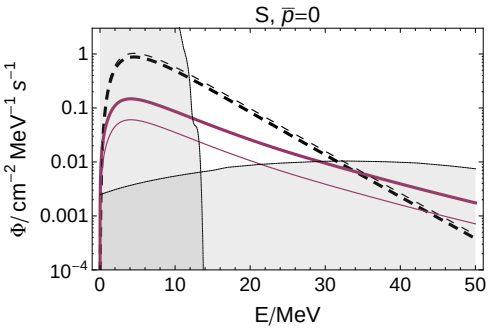

SuperK : 19.3 – 29.3 MeV

fNS	flux NS	flux BH	flux total
0.78	0.44	0.17	0.61
0.91	0.51	0.07	0.58

GADZOOKS: 11.3 – 29.3 MeV

fNS	flux NS	flux BH	flux total
0.78	2.15	0.55	2.69
0.91	2.5	0.22	2.73

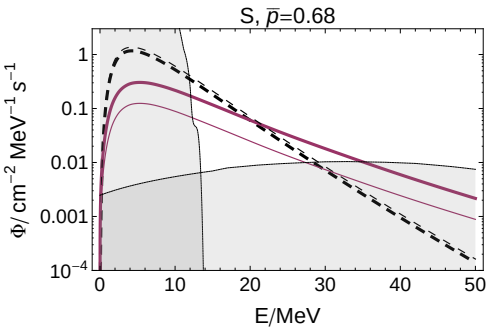

SuperK : 19.3 – 29.3 MeV

fNS	flux NS	flux BH	flux total
0.78	0.29	0.38	0.67
0.91	0.34	0.15	0.49

GADZOOKS: 11.3 – 29.3 MeV

fNS	flux NS	flux BH	flux total
0.78	1.82	1.31	3.13
0.91	2.12	0.54	2.66

FIG. 5: The diffuse flux of $\bar{\nu}_e$ from neutron star-forming collapses (dashed lines) and from failed supernovae (direct black-hole forming , solid lines). We use two different equations of state (the S EoS and the LS EoS), the extreme values for the survival probability ($\bar{p} = 0, 0.68$) and two values of the fraction of neutron star-forming collapses: $f_{NS} = 0.78$ (thick curves) and $f_{NS} = 0.91$ (thin lines). For each case we give the integrated flux in energy intervals of interest, in units of cm^{-2}s^{-1}.

on the normalization of the supernova rate, $R_{cc}(0)$. If the most conservative limit is used and all parameters are fixed to the most optimistic scenario (the largest $\Phi_{\bar{e}}^{BH}$), one gets $R_{cc}(0) < 2.1 \cdot 10^{-4}$ yr^{-1}Mpc^{-3}. Alternatively, one can fix $R_{cc}(0) = 10^{-4}$ yr^{-1}Mpc^{-3}, and obtain a constraint on the fraction of failed supernovae: $1 - f_{NS} \lesssim 0.7$, for the same set of the remaining parameters. In general, the SuperKamiokande limit excludes a small portion of the parameter space, the one where $\Phi_{\bar{e}}^{BH}$ is largest. Constraints on single quantities are loose due to degeneracies. In the future the neutrino constraints will become more powerful, when degeneracies and uncertainties are reduced by independent measurements. These could be precision tests of the supernova rate from astronomy [58, 59] or more precise NSFCs fluxes from a galactic supernova.

For the larger energy window of water with Gadolinium, $E \sim 11.3 - 29.3$ MeV, results are similar, as shown in fig. 5. We note that for the purpose of studying neutrinos from failed supernovae, the lowering of the energy threshold is not as crucial as it is for the NSFCs flux, since $\Phi_{\bar{e}}^{BH}$ emerges above $\Phi_{\bar{e}}^{NS}$ only above 20 MeV or higher. Still, the lower threshold would be important to be able to reconstruct *both* $\Phi_{\bar{e}}^{BH}$ and $\Phi_{\bar{e}}^{NS}$ individually: a fit to the lower energy data could be sufficient to reconstruct $\Phi_{\bar{e}}^{NS}$, so that the higher energy data could be used to distinguish $\Phi_{\bar{e}}^{BH}$. Besides the lower threshold, water with Gadolinium has the advantage of reducing the background in the energy window, so it can establish the DSNB with much better significance, as will be seen in the next section.

B. Events in water

Figs. 6 and 7 show the spectrum of events in 5 MeV bins of positron energy due to black hole-forming collapses, neutron star-forming collapses, and the total of the two. As expected from the $\bar{\nu}_e$ fluxes (fig. 5), the S EoS gives the largest event rate, reaching ~ 40 events per bin. The events due to failed supernovae could exceed those from NSFCs in the most fortunate case (maximum $\bar{\nu}_e$ survival and larger f_{NS}). In general, for the S EoS the contribution of failed supernovae is at least $\sim 20\%$ (10%) of the total in the $25 - 30$ (20-25) MeV bin, and could easily be at the level of 50% or so depending on the parameters. For the LS EoS the effect of failed supernovae is more modest, but still reaches $\sim 50\%$ in the $25 - 30$ MeV bin, sufficient to conclude that neutrinos from DBHFCs can not be neglected, in general.

Note that, thanks to their more energetic spectrum, the spectrum of events from black hole-forming collapses peaks in the 15-20 MeV bin, while events from neutron star-forming collapses have their maximum around or below 10 MeV. Therefore, even a modest lowering of the energy threshold would allow to capture most of the events due to DBHFCs. The expected new threshold for SuperKamiokande, $E_e \simeq 16$ MeV [18, 60], would already be sufficient.

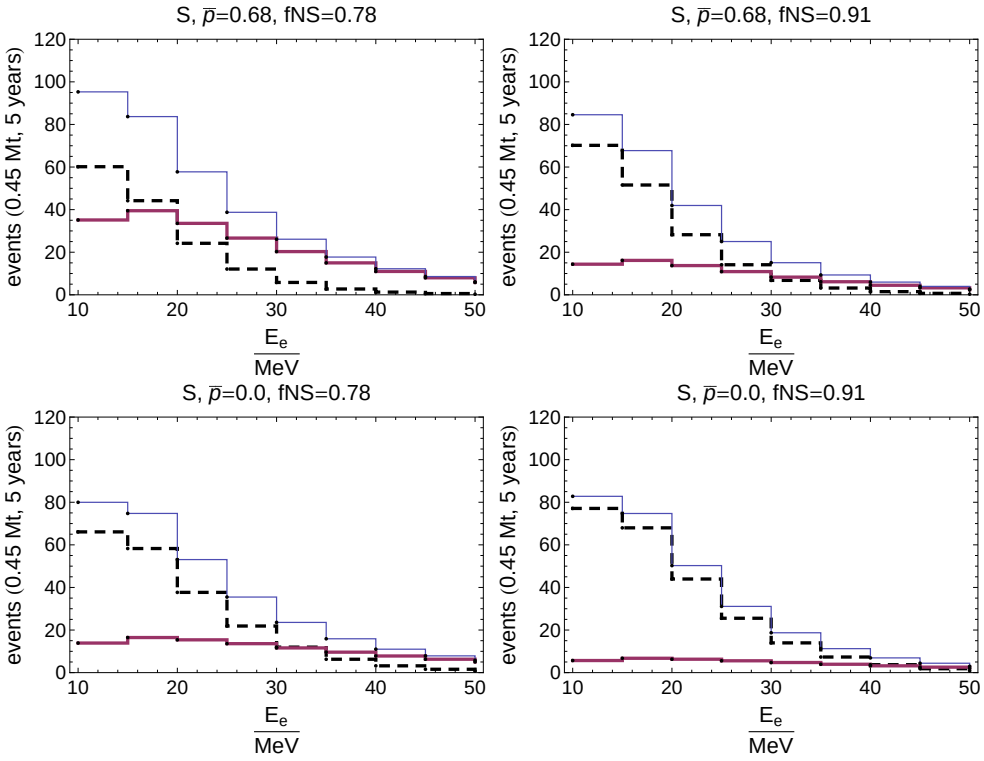

FIG. 6: The number of inverse beta decay events in a water Cherenkov detector with exposure 2.25 Mt·yr. Histograms are shown, with the S EoS, for direct black hole-forming collapses only (solid thick, purple), neutron star-forming collapses only (dashed, black), and total (solid, thin, blue).

Tables I and II give the numbers of background and signal events in water, for the S EoS and the LS EoS respectively, in different intervals of positron energy of experimental interest [75]. The total event rates exhibit the features already observed for the fluxes and for the positron energy distributions, mainly the enhancement of the signal by a factor of between $\sim 10\%$ and more than 2, compared to NSFCs only.

From the Tables one can estimate the statistical significance of the signal over the background. Following [55], we calculate the statistical error using the signal and background

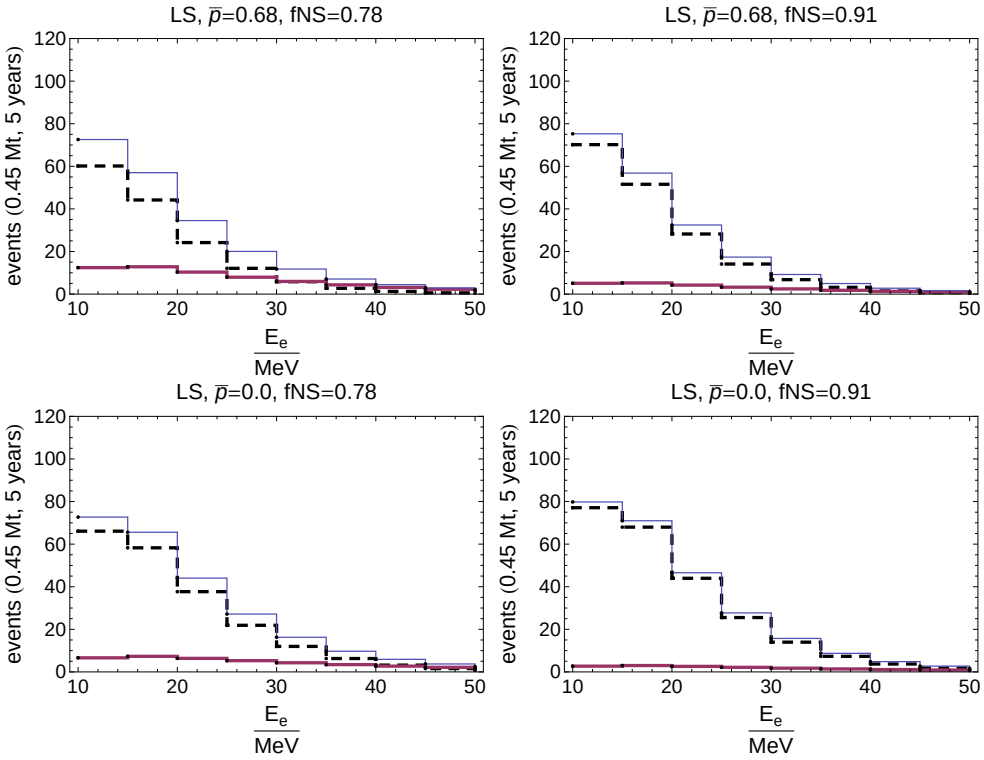

FIG. 7: The same as fig. 6, for the LS EoS.

	$\bar{p} = 0.68$			$\bar{p} = 0$			atm.	inv. muon
	NSFCs	DBHFCs	Total	NSFCs	DBHFCs	Total		
$18 < E_e/\text{MeV} < 28$	47.3 (55.2)	65.6 (26.8)	112.9 (82.0)	73.1 (85.3)	30.4 (12.4)	103.5 (97.7)	76	633
$18 < E_e/\text{MeV} < 38$	58.86 (68.68)	105.34 (43.10)	164.20 (111.78)	96.62 (112.72)	53.16 (21.75)	149.78 (134.47)	268	1675
$10 < E_e/\text{MeV} < 38$	148.33 (173.05)	164.67 (67.36)	313.00 (240.41)	200.17 (233.53)	76.97 (31.49)	277.14 (265.02)	283	1893

TABLE I: The number of signal and background events (atmospheric neutrinos and invisible muons) in a water detector of exposure 2.25 Mt·yr, in three energy windows of interest (given in terms of the positron energy, E_e), for the S EoS. The numbers of signal events are given for $\bar{p} = 0, 0.68$, $f_{NS} = 0.78$ and $f_{NS} = 0.91$ (the latter in parentheses in the table).

	$\bar{p} = 0.68$			$\bar{p} = 0$				
	NSFCs	DBHFCs	Total	NSFCs	DBHFCs	Total	atm.	inv. muon
$18 < E_e/MeV < 28$	47.3	20.2	67.5	73.1	12.5	85.6	76	633
	(55.2)	(8.3)	(63.5)	(85.3)	(5.1)	(90.4)		
$18 < E_e/MeV < 38$	58.86	31.87	90.73	96.62	20.93	117.55	268	1675
	(68.68)	(13.04)	(81.72)	(112.72)	(8.56)	(121.28)		
$10 < E_e/MeV < 38$	148.33	52.26	200.59	200.17	32.01	232.18	283	1893
	(173.05)	(21.38)	(194.43)	(233.53)	(13.10)	(246.63)		

TABLE II: The same as Table I, for the LS EoS.

rates:

$$\sigma = \sqrt{N_{sig} + N_{bckg}} \ . \tag{12}$$

and compare it with the number of events from core collapse. Note that σ is dominated by the high number of invisible muon events, and therefore is much larger than the statistical error due to the signal only [76]. For the 18-28 MeV energy window, we find that the signal has $\simeq 2.3 - 3.9\sigma$ significance, resulting in the possibility to claim detection (in absence of systematic errors) for part of the parameter space. For NSFCs only, the significance would be $\simeq 1.7 - 3\sigma$; the comparison is indicative of how the contribution of DBHFCs improves the chances of detection of the DSNB.

If the flux from NSFCs was known precisely, one could imagine analyzing the data to establish the flux from DBHFCs as a signal of its own. The number of events from failed supernovae would not be a statistically significant excess for the exposure considered here ($\sim 2.2\sigma$ at most), but would reach 3σ with about a double exposure, for the most optimistic parameters.

Using a larger window, e.g. 18-38 MeV, decreases the signal to background ratio, thus decreasing the statistical significance of the DSNB data slightly.

In the energy window $E \simeq 10 - 38$ MeV – which is viable if spallation is subtracted – the signal-to-background ratio is larger, resulting in a higher signal significance. The events due to core collapse represent a 4 - 6.3σ excess (3σ or higher for neutron star-forming collapses only) over the 2176 background events in water. A significance as high as 7.5σ is reached

for the optimized window of 10-28 MeV.

With the reduction of the invisible muon background by a factor of ~ 5, expected with Gd addition, the highest expected event rate due to DBHFCs would be significant by ~ 5 σ above the total due to the background and the flux from NSFCs, if the latter is assumed as known. However, for other flux parameters the contribution of direct black hole-forming collapses would be below 3σ and require up to three times the exposure to become significant. Our estimates on this are conservative, because they do not consider the potential of a full statistical, bin-by-bin, data analysis. In any case, every conclusion about significance is only indicative, due to the large uncertainty on the normalization of the DSNB relative to the backgrounds.

IV. NEUTRINOS: FLUX AND EVENT RATES IN LIQUID ARGON

A. ν_e flux

Let us now discuss the ν_e components of the diffuse fluxes from DBHFCs and NSFCs (Φ_e^{BH} and Φ_e^{NS}). These are shown in fig. 8, for several sets of parameters, together with the solar and atmospheric ν_e fluxes for comparison.

Overall, the ν_e fluxes are similar to the $\bar{\nu}_e$ ones. In particular, $\Phi_e = \Phi_{\bar{e}}$ if there is complete flavor permutation in both channels ($p = \bar{p} = 0$), due to the equality of the original non-electron neutrino and antineutrino fluxes for both NSFCs and DBHFCs. If $p = \bar{p} \neq 0$, the ν_e and $\bar{\nu}_e$ components of the DBHFCs flux are still nearly identical, reflecting the strong similarity of the ν_e and $\bar{\nu}_e$ fluxes at the production point (see fig. 1). In general, however, the amounts of permutation in the ν_e and $\bar{\nu}_e$ channels are expected to be different, resulting in differences between the corresponding diffuse fluxes. As in the $\bar{\nu}_e$ channel, the largest Φ_e^{BH} – in the energy window – is realized for the maximum p, the S EoS and $f_{NS} = 0.78$. Due to the stronger limit on the ν_e survival probability, $p \lesssim 0.32$, we have that $\Phi_e^{BH} \lesssim \Phi_{\bar{e}}^{BH}$. Still, for the most optimistic parameters Φ_e^{BH} dominates the total flux above ~ 26 MeV, where the signal is above the atmospheric background. For all other cases, $\Phi_e^{BH} < \Phi_e^{NS}$ in the energy window.

Looking at the fluxes integrated in the 19-29 MeV interval (fig. 8, right), we see that the flux from failed supernovae varies between $\sim 7\%$ and $\sim 50\%$ of the total flux. So, the ν_e

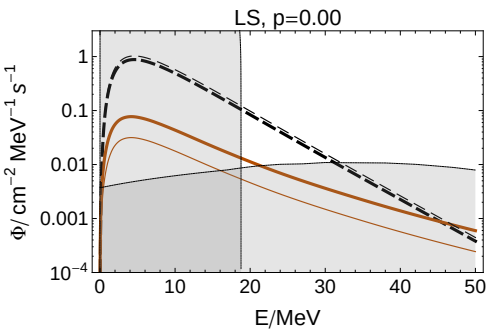

19 – 29 MeV

fNS	flux NS	flux BH	flux total
0.78	0.46	0.07	0.54
0.91	0.54	0.03	0.57

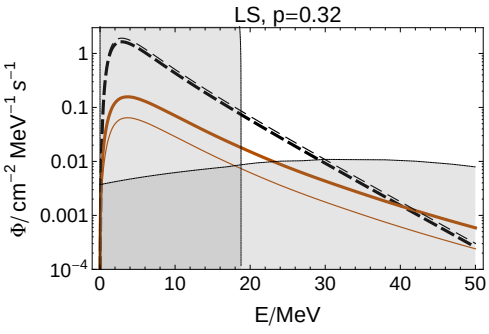

19 – 29 MeV

fNS	flux NS	flux BH	flux total
0.78	0.33	0.1	0.43
0.91	0.39	0.04	0.43

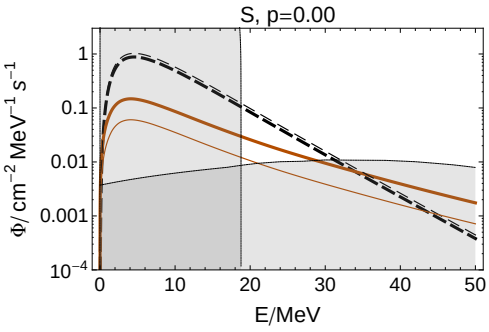

19 – 29 MeV

fNS	flux NS	flux BH	flux total
0.78	0.46	0.18	0.64
0.91	0.54	0.07	0.61

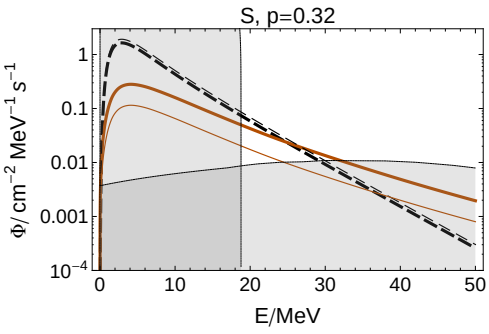

19 – 29 MeV

fNS	flux NS	flux BH	flux total
0.78	0.33	0.28	0.61
0.91	0.39	0.11	0.5

FIG. 8: The diffuse flux of ν_e from neutron star-forming collapses (dashed lines) and from failed supernovae (direct black-hole forming , solid lines). We use two different equations of state (the S EoS and the LS EoS), the extreme values for the survival probability ($p = 0, 0.32$) and two values of the fraction of neutron star-forming collapses: $f_{NS} = 0.78$ (thick lines) and $f_{NS} = 0.91$ (thin). For each case, we give the integrated flux in the energy interval of interest, in units of $\mathrm{cm}^{-2}\mathrm{s}^{-1}$.

component of the DSNB could be doubled by the contribution of DBHFCs – reaching the value of $\sim 0.64\ \mathrm{s^{-1}cm^{-2}}$ – or be only moderately affected by it, depending on the parameters.

B. Events in liquid argon

In figs. 9 and 10 we show the expected event distributions (in neutrino energy) for a LAr experiment with 0.5 Mt $\cdot$ yr exposure, for several sets of parameters.

In contrast with a water detector, here the events from DBHFCs peak inside the detector energy window (or even slightly beyond, for the S EoS with $p = 0$), $E \sim 19 - 30$ MeV, and not below it, thanks to the faster increase of the detection cross section with energy. Instead, the peak of the events from NSFCs is below 19 MeV and therefore it is obscured by solar neutrinos. Thus, the LAr technology, while needing threshold improvement to probe the bulk of NSFCs events, is suitable as it is to study failed supernovae. For these, the most important improvement will probably be at the high end of the energy window, where the atmospheric background is the limiting factor.

For the numbers of events, figs. 9 and 10 confirm what was already observed for the fluxes: the contribution of failed supernovae to the signal ranges from modest to dominant. Specifically, the DBHFCs contribute to each energy bin by at least $\sim 7\%$, and by more than $\sim 25\%$ for most of the parameter space. Considering the low statistics, these excesses would probably be marginally significant at best, once theoretical uncertainties – especially on normalizations – are included. Still, the inclusion of failed supernovae in the modeling of the signal would be important to have a reliable prediction as benchmark, and to estimate the theoretical error correctly.

Tables III and IV give the numbers of events expected for different sets of parameters and different energy intervals. We see that, for the S EoS and the interval $19 - 39$ MeV, failed supernovae increase the event rate by $\sim 30 - 100\%$; specifically, the number of events goes from $\sim 8 - 12$ to $\sim 14 - 20$. With $\sim 8 - 9$ background events expected, the significance of the signal changes from $\sim 2.3 - 3\sigma$ to $\sim 3 - 3.7\sigma$. In the assumption of known Φ_e^{NS}, the number of events due to Φ_e^{BH} would be too small to be significant as a signal of its own, giving an excess of less than 1.7σ. For the largest Φ_e^{BH}, a 3σ excess would be realized for a triple exposure, 1.5 Mt$\cdot$yr.

For the smaller window $19 - 29$ MeV, the signal to background ratio increases, but the

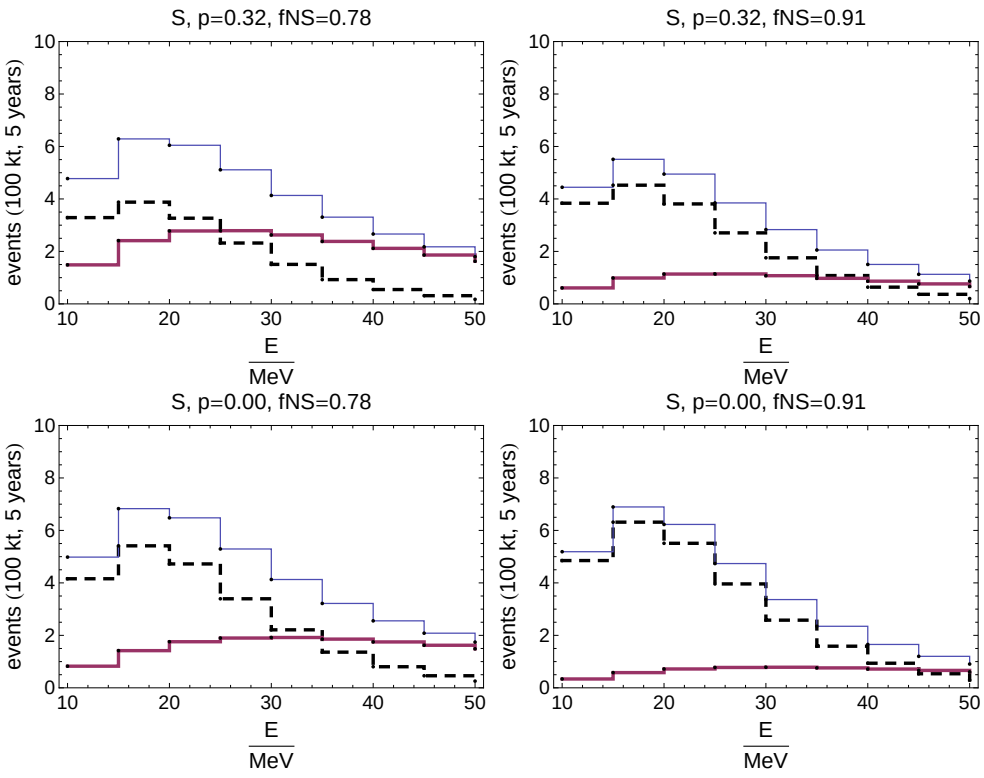

FIG. 9: The number of ν_e events in a liquid argon detector with exposure 0.5 Mt·yr, for different sets of parameters. Histograms are shown,using the S EoS, for direct black hole-forming collapses only (solid thick, purple), neutron star-forming collapses only (dashed, black), and total (solid, thin, blue).

lower statistics compensate for this advantage, so that the significance of the signal due to the total DSNB becomes slightly worse, reaching 3σ in the most fortunate case.

For the LS EoS we expect ~ 12 events from the DSNB in the window $19 - 39$ MeV; of these $1 - 3$ events would be from failed supernovae. These are not significant as a signal, but contribute to enhancing the statistical significance of the total number of events. This reaches $\sim 2.7\sigma$ at most, so that a significant excess could be established above the background with a moderately larger exposure. The significance is lower if the energy window is restricted, as observed previously.

The enhancement of the signal due to failed supernovae implies that a smaller exposure will be necessary (compared to NSFCs only) for detection, therefore allowing a smaller mass and/or running time. For example, for the most favourable set of parameters, a 10 kt detector running for 5 years and searching in the $19 - 39$ MeV window could see about 2

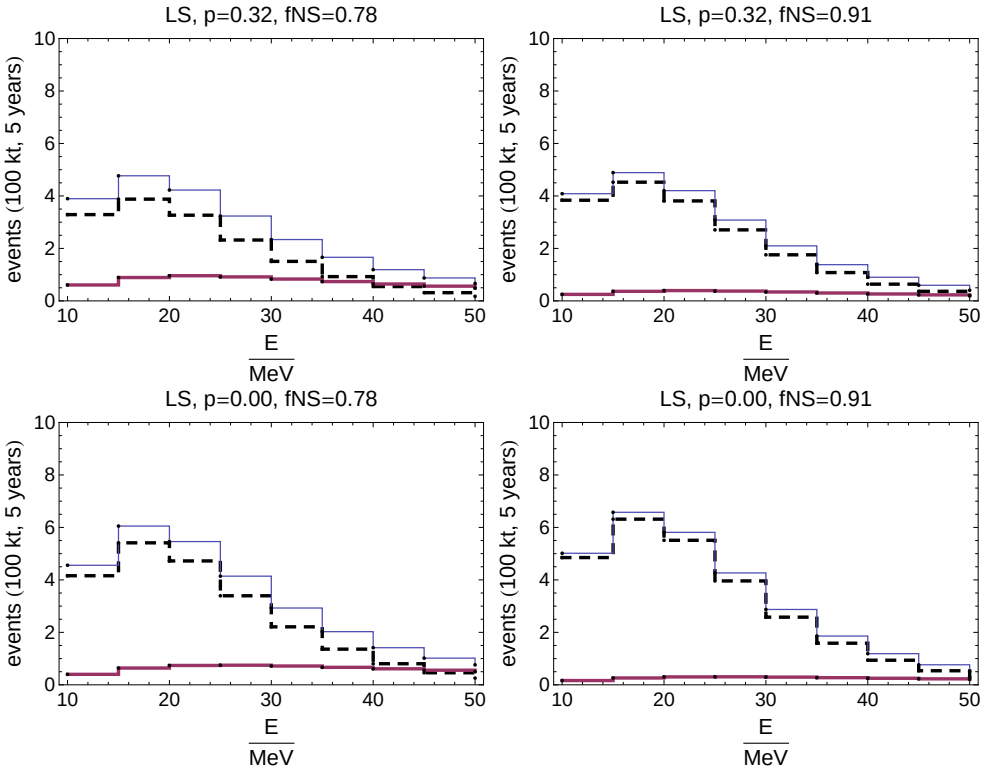

FIG. 10: The same as fig. 9 for the LS EoS.

	$p = 0.32$			$p = 0$			
	NSFCs	DBHFCs	Total	NSFCs	DBHFCs	Total	atm.
$19 < E/\text{MeV} < 29$	5.9 (6.9)	5.5 (2.3)	11.5 (9.2)	8.6 (10.0)	3.6 (1.5)	12.2 (11.5)	2.25
$19 < E/\text{MeV} < 39$	8.6 (10.0)	10.6 (4.4)	19.3 (14.4)	12.5 (14.6)	7.4 (3.0)	19.9 (17.6)	8.6
$10 < E/\text{MeV} < 39$	15.0 (17.5)	14.0 (5.7)	29.0 (23.3)	21.0 (24.5)	9.3 (3.8)	30.3 (28.4)	9.0

TABLE III: The number of ν_e interactions on ^{40}Ar from the DSNB and from atmospheric neutrinos, in three energy windows of interest (given in terms of the neutrino energy, E) at a liquid argon detector of 0.5 Mt·yr exposure. The rates for DBHFCs refer to the S EoS, $f_{NS} = 0.78$ and $f_{NS} = 0.91$ (the latter in parentheses).

	$p = 0.32$			$p = 0$			
	NSFCs	DBHFCs	Total	NSFCs	DBHFCs	Total	atm.
$19 < E/\mathrm{MeV} < 29$	5.9	1.9	7.8	8.6	1.5	10.1	2.25
	(6.9)	(0.8)	(7.7)	(10.0)	(0.6)	(10.6)	
$19 < E/\mathrm{MeV} < 39$	8.6	3.5	12.1	12.5	2.9	15.4	8.6
	(10.0)	(1.4)	(11.5)	(14.6)	(1.2)	(15.8)	
$10 < E/\mathrm{MeV} < 39$	15.0	4.8	19.8	21.0	9.3	24.8	9.0
	(17.5)	(2.0)	(19.5)	(24.5)	(1.5)	(26.1)	

TABLE IV: The same as Table III for the LS EoS.

events from core collapses, compared to less than 1 from background and less than 1 expected from NSFCs only. This is encouraging, in principle, although errors would be insufficient to make firm conclusions in this case.

V. DIRECTIONS OF FURTHER STUDY

Our results are limited by the still incomplete investigation of neutrino emission from failed supernovae and from all collapses in general. As these progress, a number of aspects will be included in the calculation of the diffuse flux. Here we discuss them briefly.

- Dependence on the EoS. Little exists beyond the results with the LS and S EoS that we have used here for failed supernovae. However, initial studies evidence some trends. Stiffer equations of state correspond to longer neutrino emission [10, 61], and therefore to a more luminous time-integrated flux and diffuse flux. The effect of the EoS is stronger for DBHFCs than for NSFCs, where differences are mostly in the neutrino average energies and at the level of $\sim 10\%$ or so [61]. It has to be stressed, though, that most results for NSFCs refer to the first second post-bounce, while a full, ~ 10 s simulation is required to model the diffuse flux. Progress in this direction exists [62, 63], but is still without systematic exploration of the EoS dependence. Due to this lack of information, here we have neglected the EoS dependence of the NSFCs diffuse flux.

Equations of state involving quarks, hyperons and/or pions have been considered for failed supernovae [14, 42, 64]: they tend to shorten the neutrino emission and thus to decrease the diffuse flux. Pions, however, tend to increase the luminosity and average energy of the neutrino spectrum. Effects are of the order of tens of per cent, so they may be difficult to distinguish in the diffuse flux.

- Effects of fallback black hole forming collapses (FBHFCs). Ultimately, a robust prediction of the DSNB will require modeling the whole continuum between neutron star formation and direct black hole formation, with the inclusion of the intermediate case of black hole formation by fallback, which is expected for at least some of the progenitors in the mass interval $\sim 25 - 40$ $M_\odot$. For FBHFCs, the initially formed neutron star collapses into a black hole as a result of accretion, after an explosion. The explosion becomes weaker with the increase of the progenitor mass, until FBHFCs become indistinguishable from DBHFCs. For FBHFCs with a robust explosion, the neutrino emission resembles that of a neutron-star forming collapse for the first 10-20 s, and then exhibits a characteristic increase of the neutrino luminosity at later times as an effect of fallback [65, 66]. This phenomenon was studied in a set of numerical simulations [65], and was found to contribute by about $\sim 10\%$ to the total (time-integrated) neutrino flux. However, the same simulations are still inconclusive about whether a black hole eventually forms, and systematic studies of heavy fallback for very massive progenitors are still needed to reach firm conclusions.

- Effects of the diverse stellar population. It is fascinating that the DSNB receives contributions from an enormous variety of stars, which may differ in many parameters like progenitor mass, magnetic fields, metallicity, rotation, etc. The dependence of failed supernovae on at least some of these parameters has been studied recently. Studies with different models of progenitor stars in the 40-50 $M_\odot$ interval [13] have shown that different stellar density profiles could result in very different oscillation effects, within the intervals in eq. (5), while differences in the produced (pre-oscillation) neutrino fluxes are likely to be minor compared to the several uncertainties in the problem [12]. A detailed study of direct black hole collapse with and without rotation [45] has shown that rotation tends to prevent or delay the black hole formation, with overall lower neutrino luminosities and average energies. The same study predicts that up to 15%

of low metallicity stars (metallicity less than 10^{-4} times that of our Sun) can undergo direct black hole formation, compared to the maximum of $\sim 7\%$ for stars with solar metallicity. Therefore, one might expect an enhanced contribution to the DSNB from low metallicity stars. However, this enhancement is probably overcompensated by the relative rarity of such stars at low redshift.

Finally, we recall that some failed supernovae may generate collapsars, the hosts of the Gamma Ray Bursts (and their accompanying jets of $\sim$ TeV neutrinos). These collapsars continue to emit $\mathcal{O}(10)$ MeV neutrinos after the black hole formation, due to the presence of an accretion disk around the black hole itself [67, 68]. While very luminous, this neutrino flux should contribute to the DSNB at the level of $\sim 10\%$ or less, due to the rarity of collapsars, see e.g., [67].

VI. DISCUSSION AND CONCLUSIONS

Let us summarize our results.

- The diffuse flux from DBHFCs reflects the features of the original neutrino flux from a failed supernova: it is more luminous and more energetic than the flux from neutron star-forming collapses, with the most energetic spectra being realized for the stiffer, Shen et al. equation of state. In energy windows relevant for detection, the $\bar{\nu}_e$ component of this flux is at a maximum for the largest $\bar{\nu}_e$ survival probability, due to the especially large flux of $\bar{\nu}_e$s originally produced in the star. An analogous result holds for the ν_e component as well. This contrasts with the case of neutron star-forming collapses, where the luminosity is roughly equipartitioned among the neutrino species.

- Because of its more energetic spectrum, the flux from DBHFCs has a cosmological component – from stars with $z \gtrsim 1$ – as large as $\sim 40\%$ above 20 MeV. This is interestingly larger than the $\sim 10\%$ or less expected in the same interval for NSFCs, for which the cosmological component largely accumulates below the experimental energy threshold. This could result in new possibilities to use neutrinos to test the rate of collapses at cosmological distances.

- The harder spectrum of the DBHFCs flux can result in a wider energy window of detection for the DSNB (defined as the energy interval where the core collapse flux

exceeds the background fluxes of neutrinos of other origin). The window can be up to roughly 7 MeV wider than for NSFCs only, depending on the magnitude of the atmospheric background relative to the signal (fig. 4).

- The diffuse flux of neutrinos from failed supernovae could be substantial, up to $\phi_{\bar{e}}^{BH} = 0.38\ \ \mathrm{s^{-1}cm^{-2}}$ ($\phi_{e}^{BH} = 0.28\ \ \mathrm{s^{-1}cm^{-2}}$) for $\bar{\nu}_e$ (ν_e) in the interval $19.3 - 29.3$ MeV, normalized to a local rate of core collapses of $R_{cc}(0) = 10^{-4}\ \mathrm{yr^{-1}Mpc^{-3}}$. This is only a factor of ~ 4 lower than the current sensitivity of SuperKamiokande, indicating the possibility of detection in the near future.

- Depending on the parameters (the oscillation probabilities, the fraction of black hole-forming collapses and the EoS), the flux from failed supernovae ranges from 6-10% to a dominant fraction of the total DSNB, for energies of experimental interest. The total flux is enhanced – compared to neutron star-forming collapses only – by up to a factor ~ 2.3, reaching $\phi_{\bar{e}} \simeq 0.67\ \ \mathrm{s^{-1}cm^{-2}}$ in the $19.3 - 29.3$ MeV window, and $\phi_{\bar{e}}^{BH} = 0.89\ \ \mathrm{s^{-1}cm^{-2}}$ in the open interval $E > 19.3$ MeV. The latter estimate is only a factor of ~ 2 lower than of the current SuperKamiokande limit, Eq. (10), and therefore it is very promising for the next phase of experimental searches.

- The SuperKamiokande limit constrains the multi-dimensional region of the parameter space. This loose constraint can be expressed in terms of conditional limits on the individual parameters: for example, the rate of core collapses is constrained to $R_{cc}(0) < 2.1 \cdot 10^{-4}\ \mathrm{yr^{-1}Mpc^{-3}}$ when all the other parameters are fixed to maximize $\Phi_{\bar{e}}^{BH}$. Similarly, one gets a limit on the fraction of failed supernovae, $f_{BH} = 1 - f_{NS} \lesssim 0.7$, for the same set of parameters and $R_{cc}(0) = 10^{-4}\ \mathrm{yr^{-1}Mpc^{-3}}$.

- in a detector, the most immediate effect of the neutrino flux from DBHFCs is an enhancement of the event rate, which reflects the enhancement of the flux compared to neutron star-forming collapses only. In a water Cherenkov detector with a 2.25 Mt·yr exposure (e.g., 0.45 Mt for 5 years) we expect $\sim 5 - 65$ events from failed supernovae in the window 18-28 MeV of positron energy, out of a total of 63-113 events from all collapses. These represent an excess of $2.3 - 3.9\sigma$, after background rates have been included to calculate errors. For the extended window 10-38 MeV, relevant to water plus Gadolinium, we get 13-165 events from failed supernovae and

a total of $\sim 190 - 310$ events from all collapses, corresponding to an excess of 4 - 6σ above background.

- in liquid argon the spectrum of events from DBHFCs peaks above $\sim$ 19 MeV, where the solar neutrino flux terminates. This is a distinctive feature of liquid argon, and is due to the fast increase of the cross section with the neutrino energy.

- For a liquid argon detector with exposure of 0.5 Mt·yr, the larger energy window of 19-39 MeV is overall convenient to increase statistics at the price of a slightly worse signal-to-background ratio. For this window we predict 1-11 events from DBHFCs, and a total of 12-20 signal events, with 9 events from background. Statistical significance of 3σ is realized for the S EoS, in the absence of background systematics.

Our results show that, with an improvement by a factor of 2 (in flux) of its sensitivity, SuperKamiokande can start to probe the parameter space of neutrinos from failed supernovae at the basic level and that next generation detectors should cover a substantial portion of this space.

Due to uncertainties in the normalizations, the most robust signature of failed supernovae in the diffuse flux would be the harder spectrum, and possibly a deviation from the characteristic exponential shape of the spectrum of the DSNB [69] where the two contributions, from neutron star-forming and black hole-forming collapses, are comparable. Such spectral distortion could be visible with the extended energy window of a water+Gd detector or with a liquid scintillator detector [47], which both have the advantage of a better energy resolution.

To establish the presence of a flux from failed supernovae would already be a fundamental result, being the first detection of new type of neutrino source. Beyond the discovery phase, with a high statistics signal it might be possible to distinguish between different models of black hole-forming collapse, at the level of favouring one EoS over another, although a model-independent discrimination might not be possible due to the large errors. The cases with the largest Φ^{BH} – maximum survival of the electron flavors and smallest f_{NS} – might be established or ruled out relatively easily, while other scenarios might be more difficult to probe because their lower flux is more shadowed by the atmospheric background.

For a given model of neutrino spectra from black hole-forming and neutron star-forming collapses, the position of the spectral distortion (with respect to an exponential spectrum)

might be used to probe the relative frequency of the two types, in other words f_{NS}, and in turn the minimum progenitor mass required to produce a direct black hole-forming collapse (sec. II). It is likely that in the space of a few years the rate of neutron star-forming collapses will be known with good precision from astronomy [58, 59], and this will allow translation of the information on f_{NS} obtained from neutrinos into an absolute (as opposed to relative) rate of failed supernovae.

Data on neutrinos from failed supernovae would also constitute a new ground to test neutrino oscillations, and therefore neutrino masses and mixings. Realistically, only average survival probabilities could be extracted from a fit to high statistics data. It would be especially interesting to look for differences in the oscillation patterns for DBHFCs and NSFCs, as these could give insight on the different physics at play in the two types of collapses (e.g., different matter density profiles influencing the MSW resonances).

To conclude, the detection of a diffuse neutrino flux from failed supernovae is a realistic possibility. It would have profound implications on the study of these invisible objects, on which we have no data so far. The flux is uncertain by more than one order of magnitude, and therefore it remains to be established whether it dominates the total flux or just modifies it at the 10% level. In the first case, a change of perspective in the field will be needed. In the latter, failed supernovae would be an ingredient of precision modeling of the DSNB and their parameter space would be constrained experimentally.

Acknowledgments

We are grateful to G. Mangano and M. Vagins for useful exchanges. C.L. acknowledges the support of the NSF under Grant No. PHY-0854827. J.G.K. acknowledges the resources available to him at Arizona State University during his undergraduate studies.

---

[1] K. Hirata et al. (KAMIOKANDE-II), Phys. Rev. Lett. **58**, 1490 (1987).

[2] R. M. Bionta et al., Phys. Rev. Lett. **58**, 1494 (1987).

[3] M. Malek et al. (Super-Kamiokande), Phys. Rev. Lett. **90**, 061101 (2003), hep-ex/0209028.

[4] K. Eguchi et al. (KamLAND), Phys. Rev. Lett. **92**, 071301 (2004), hep-ex/0310047.

[5] B. Aharmim et al. (SNO Collaboration), Astrophys.J. **653**, 1545 (2006), hep-ex/0607010.

[6] C. Lunardini and O. L. Peres, JCAP **0808**, 033 (2008), 0805.4225.

[7] K. Sumiyoshi, S. Yamada, H. Suzuki, and S. Chiba, Phys. Rev. Lett. **97**, 091101 (2006), astro-ph/0608509.

[8] C. Lunardini, Phys. Rev. Lett. **102**, 231101 (2009), 0901.0568.

[9] M. Liebendoerfer et al., Astrophys. J. Suppl. **150**, 263 (2004), astro-ph/0207036.

[10] K. Sumiyoshi, S. Yamada, and H. Suzuki, Astrophys.J. **667**, 382 (2007), 0706.3762.

[11] T. Fischer, S. C. Whitehouse, A. Mezzacappa, F. K. Thielemann, and M. Liebendorfer, Astron. Astrophys. **499**, 1 (2009), 0809.5129.

[12] K. Sumiyoshi, S. Yamada, and H. Suzuki, Astrophys. J. **688**, 1176 (2008), 0808.0384.

[13] K. Nakazato, K. Sumiyoshi, H. Suzuki, and S. Yamada, Phys. Rev. **D78**, 083014 (2008), 0810.3734.

[14] K. Nakazato, K. Sumiyoshi, and S. Yamada, Astrophys. J. **721**, 1284 (2010), 1001.5084.

[15] J. F. Beacom and M. R. Vagins, Phys. Rev. Lett. **93**, 171101 (2004), hep-ph/0309300.

[16] A. Lien, B. D. Fields, and J. F. Beacom, Phys. Rev. **D81**, 083001 (2010), 1001.3678.

[17] T. Iida, J. Phys.: Conf. Ser. **136**, 042075 (2005).

[18] T. Iida, phD thesis, U. of Tokyo, 2010. Available at http://www-sk.icrr.u-tokyo.ac.jp/sk/pub/.

[19] R. Lazauskas, C. Lunardini, and C. Volpe, JCAP **0904**, 029 (2009), 0901.0581.

[20] R. N. Boyd, T. Kajino, and T. Onaka, Astrobiology **10**, 561 (2010), 1001.3849.

[21] A. M. Hopkins and J. F. Beacom, Astrophys. J. **651**, 142 (2006), astro-ph/0601463.

[22] S. E. Woosley, A. Heger, and T. A. Weaver, Rev. Mod. Phys. **74**, 1015 (2002).

[23] E. E. Salpeter, Astrophys. J. **121**, 161 (1955).

[24] M. T. Keil, G. G. Raffelt, and H.-T. Janka, Astrophys. J. **590**, 971 (2003), astro-ph/0208035.

[25] A. Heger, C. L. Fryer, S. E. Woosley, N. Langer, and D. H. Hartmann, Astrophys. J. **591**, 288 (2003), astro-ph/0212469.

[26] S. E. Woosley and T. Weaver, Astrophys. J. Suppl. 101, 181 (1995).

[27] H. Shen, H. Toki, K. Oyamatsu, and K. Sumiyoshi, Nucl. Phys. A **637**, 435 (1998).

[28] J. M. Lattimer and F. D. Swesty, Nucl. Phys. A **535**, 331 (1991).

[29] A. S. Dighe and A. Y. Smirnov, Phys. Rev. **D62**, 033007 (2000), hep-ph/9907423.

[30] B. Dasgupta and A. Dighe, Phys. Rev. **D77**, 113002 (2008), 0712.3798.

[31] C. Lunardini and A. Y. Smirnov, JCAP **0306**, 009 (2003), hep-ph/0302033.

[32] H. Duan, G. M. Fuller, and Y.-Z. Qian, Phys. Rev. **D74**, 123004 (2006), astro-ph/0511275.

[33] S. Hannestad, G. G. Raffelt, G. Sigl, and Y. Y. Y. Wong, Phys. Rev. **D74**, 105010 (2006), astro-ph/0608695.

[34] G. G. Raffelt and A. Y. Smirnov, Phys.Rev. **D76**, 081301 (2007), 0705.1830.

[35] A. Esteban-Pretel, S. Pastor, R. Tomas, G. G. Raffelt, and G. Sigl, Phys.Rev. **D76**, 125018 (2007), 0706.2498.

[36] G. L. Fogli, E. Lisi, A. Marrone, and A. Mirizzi, JCAP **0712**, 010 (2007), 0707.1998.

[37] H. Duan and J. P. Kneller, J.Phys.G **G36**, 113201 (2009), arXiv:0904.0974.

[38] H. Duan, G. M. Fuller, J. Carlson, and Y.-Q. Zhong, Phys. Rev. Lett. **99**, 241802 (2007), 0707.0290.

[39] B. Dasgupta, A. Dighe, G. G. Raffelt, and A. Y. Smirnov, Phys.Rev.Lett. **103**, 051105 (2009), arXiv:0904.3542.

[40] G. Fogli, E. Lisi, A. Marrone, and I. Tamborra, JCAP **0910**, 002 (2009), arXiv:0907.5115.

[41] A. Friedland, Phys.Rev.Lett. **104**, 191102 (2010), arXiv:1001.0996.

[42] K. Nakazato, K. Sumiyoshi, H. Suzuki, and S. Yamada, Phys.Rev. **D81**, 083009 (2010), arXiv:1004.0291.

[43] S. Ando and K. Sato, New J. Phys. **6**, 170 (2004), astro-ph/0410061.

[44] S. J. Smartt, J. J. Eldridge, R. M. Crockett, and J. R. Maund, Mon. Not. Roy. Astron. Soc. **395**, 1409 (2009), 0809.0403.

[45] E. O'Connor and C. D. Ott, Astrophys. J. **730**, 70 (2011), 1010.5550.

[46] G. Battistoni, A. Ferrari, T. Montaruli, and P. R. Sala, Astropart. Phys. **23**, 526 (2005).

[47] M. Wurm et al., Phys. Rev. **D75**, 023007 (2007), astro-ph/0701305.

[48] DUSEL white paper, in preparation. Available at http://citeseerx.ist.psu.edu/viewdoc/summary?doi=10.1.1.156.7734.

[49] M. Vagins, private communication.

[50] K. A. Hochmuth et al., Astropart. Phys. **27**, 21 (2007), hep-ph/0509136.

[51] A. Terashima et al. (KamLAND), J. Phys. Conf. Ser. **120**, 052029 (2008).

[52] J. N. Bahcall, A. M. Serenelli, and S. Basu, Astrophys. J. **621**, L85 (2005), astro-ph/0412440.

[53] C. Lunardini (2010), arXiv:1007.3252.

[54] A. Strumia and F. Vissani, Phys. Lett. **B564**, 42 (2003), astro-ph/0302055.

[55] G. L. Fogli, E. Lisi, A. Mirizzi, and D. Montanino, JCAP **0504**, 002 (2005), hep-ph/0412046.

[56] A. G. Cocco, A. Ereditato, G. Fiorillo, G. Mangano, and V. Pettorino, JCAP **0412**, 002

(2004), hep-ph/0408031.

[57] E. Kolbe, K. Langanke, G. Martinez-Pinedo, and P. Vogel, J. Phys. **G29**, 2569 (2003), nucl-th/0311022.

[58] SNAP letter of intent, at http://snap.lbl.gov/ (2004).

[59] SNLS collaboration, http://www.cfht.hawaii.edu/SNLS/ (2010).

[60] M. Smy (2009), talk at the workshop *Supernova Physics and DUSEL*, Los Angeles.

[61] M. Hempel, T. Fischer, J. Schaffner-Bielich, and M. Liebendorfer (2011), 1108.0848.

[62] T. Fischer, S. C. Whitehouse, A. Mezzacappa, F. K. Thielemann, and M. Liebendorfer, Astron. Astrophys. **517**, A80 (2010), 0908.1871.

[63] L. Hudepohl, B. Muller, H. T. Janka, A. Marek, and G. G. Raffelt, Phys. Rev. Lett. **104**, 251101 (2010), 0912.0260.

[64] K. Nakazato, S. Furusawa, K. Sumiyoshi, A. Ohnishi, S. Yamada, et al. (2011), 1111.2900.

[65] C. L. Fryer, Astrophys. J. **699**, 409 (2009), 0711.0551.

[66] C. L. Fryer et al., Astrophys. J. **707**, 193 (2009), 0908.0701.

[67] S. Nagataki, K. Kohri, S. Ando, and K. Sato, Astropart. Phys. **18**, 551 (2003), astro-ph/0203481.

[68] G. C. McLaughlin and R. Surman, Phys. Rev. **D75**, 023005 (2007), astro-ph/0605281.

[69] C. Lunardini, Phys. Rev. **D75**, 073022 (2007), astro-ph/0612701.

[70] C. S. Kochanek et al., Astrophys. J. **684**, 1336 (2008), 0802.0456.

[71] An interesting possibility has been suggested recently [70]: observing the disappearance of stars rather than the appearance of supernovae. In principle, a "before vs after" comparison, together with the non-observation of a supernova explosion, could reveal a direct black hole-forming collapse.

[72] The bumps at 20-30 MeV in the lower curves of fig. 2 are a numerical artifact due to interpolating a sparse set of points in the highest energy part of the original spectra (fig. 1). Therefore, these curves have indicative value only.

[73] Water detectors are sensitive to solar neutrinos via neutrino-electron scattering. However, these events can be effectively subtracted because they are highly directional. This is not the case for ν_e charged current scattering on ^{40}Ar, therefore solar neutrino events will have to be included in the data analysis of LAr detectors.

[74] We quote the limit as given in [6] for a large variety of neutrino spectra and with an updated

inverse beta decay cross section. The limit given by the SuperKamiokande collaboration in 2002 is $\phi_{\bar{e}}(E)(E > 19.3 \text{ MeV}) < 1.2 \text{ cm}^{-2}\text{s}^{-1}$ at 90% C.L. [3]. It remains to be determined what the limit is for the more energetic spectrum of neutrinos from failed supernovae (see [17, 18] for preliminary results).

[75] For generality, all the background event rates refer to pure water, and do not include the expected reduction of the invisible muon events allowed by water+Gadolinium, which depends on the specific detector design and therefore is uncertain. As discussed in sec. II C, a reduction of a factor of ~ 5 is expected.

[76] The systematic uncertainties on the background rates are probably minor compared to the purely statistical errors. Indeed, the atmospheric neutrino flux has about 20%-40% systematic uncertainty [46], which translates into a ∼10-20% effect on σ. Moreover, the normalization of the invisible muon event rate is known from the analysis of the SuperKamiokande data, and therefore is constrained within tens of per cent uncertainty [3].